

Design and Fabrication of a Micropillar-Pumped Polymer Loop Heat Pipe

Masaaki Hashimoto¹, Taiga Kawakami¹, Abdulkareem Alasli², Ryobu Nomura¹, Hosei Nagano¹, and Ai Ueno¹

Abstract—This letter presents a micropillar-pumped polymer loop heat pipe (LHP) with potential applications in flexible electronics. A unique evaporator with a micro pillar wick was designed for a flexible polymer LHP. The polymer LHP was fabricated via simple and cost-effective soft lithography, omitting the need for a porous wick. This design and fabrication approach facilitated passive two-phase cooling in the polymer LHP, with up to 34 °C reduction in evaporator temperature when compared to a non-fluid-charged state in a horizontal orientation. [2023-0140]

Index Terms—Flexible electronics, micropillar wick, polymer loop heat pipe, two-phase heat transfer.

I. INTRODUCTION

RECENTLY, polymer two-phase heat transfer devices have attracted substantial attention for their potential applications in flexible electronics. Heat pipes (HPs) and loop HPs (LHPs) are passive two-phase heat transfer devices that exploit the latent heat of the evaporated working fluid for heat transport. Polymer HPs and LHPs exhibit the advantages of flexibility, low weight, low cost, electrical insulation, and chemical resistance. Although many polymer HPs have been proposed [1], [2], [3], [4], [5], [6], polymer LHPs have been rarely reported owing to challenges in their design and fabrication.

An LHP comprises an evaporator, a vapor line, a condenser, a liquid line, and a compensation chamber. The evaporator includes a wick that unidirectionally pumps the working fluid from the compensation chamber, enabling longer-range heat transfer than that possible using HPs. Designing and fabricating an evaporator using flexible polymer materials are the major challenges in polymer LHP fabrication. To prevent bidirectional flow or inverse vapor leakage from the evaporator, resulting in the failure of the LHP operation, the interface between the wick and compensation chamber must be sufficiently sealed [7], [8]. The evaporator of a nonpolymer LHP is typically constructed using rigid metal materials. To ensure the sealing of the evaporator section, the porous wick is firmly sandwiched within rigid metal cases with close interfacial contact [9], [10], [11]. However, in polymer LHPs, this approach is precluded by poor interfacial contact between the flexible polymer material and porous wick.

This letter presents the design and fabrication of a micropillar-pumped polymer LHP. A unique evaporator with a micropillar wick is designed for a flexible polymer LHP. The polymer LHP is fabricated via simple and cost-effective soft lithography with no porous wick.

Manuscript received 5 August 2023; revised 8 September 2023; accepted 14 September 2023. Date of publication 20 October 2023; date of current version 1 December 2023. This work was supported in part by the Asahi Glass Foundation and in part by the Japan Society for the Promotion of Science KAKENHI under Grant JP22K03943. Subject Editor S. Rajaraman. (Corresponding author: Ai Ueno.)

Masaaki Hashimoto is with the Department of System Design Engineering, Keio University, Yokohama, Kanagawa 223-8522, Japan (e-mail: hashimoto@sd.keio.ac.jp).

Taiga Kawakami, Abdulkareem Alasli, Ryobu Nomura, Hosei Nagano, and Ai Ueno are with the Department of Mechanical System Engineering, Nagoya University, Nagoya, Aichi 464-8603, Japan (e-mail: ueno@mech.nagoya-u.ac.jp).

Color versions of one or more figures in this article are available at <https://doi.org/10.1109/JMEMS.2023.3318413>.

Digital Object Identifier 10.1109/JMEMS.2023.3318413

© 2023 The Authors. This work is licensed under a Creative Commons Attribution-NonCommercial-NoDerivatives 4.0 License.

For more information, see <https://creativecommons.org/licenses/by-nc-nd/4.0/>

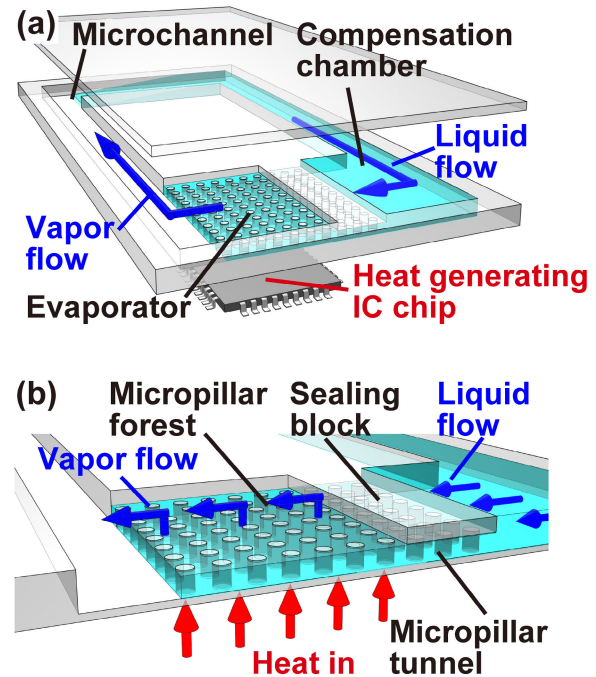


Fig. 1. Design concept of a micropillar-pumped polymer loop heat pipe: (a) perspective view of the device and (b) cross-sectional view of the evaporator section.

The sealing of the evaporator is enabled by partially-cured bonding of two polydimethylsiloxane (PDMS) films. Our design and fabrication approaches are expected to realize polymer LHPs for flexible electronics.

II. DESIGN CONCEPT AND FABRICATION

Fig. 1 illustrates the design concept of a micropillar-pumped polymer LHP. The LHP is designed to dissipate heat from an integrated circuit (IC) chip in flexible electronic devices. The liquid in the micropillar forest is pumped from the compensation chamber and conductively heated to a vapor from the bottom side of the case. The menisci formed in the micropillar forest generate capillary forces that push the vapor into the microchannel. The capillary forces depend on the micropillar geometry, which primarily determines the heat transfer length. The capillary force P of the micropillar wick can be calculated as follows [12]:

$$P = 4\sigma \cos \theta / D \left(\frac{4}{\pi} \left(\frac{L}{D} \right)^2 - 1 \right), \quad (1)$$

where σ is the liquid–vapor surface tension, θ is the receding contact angle of liquid meniscus, L is the center-to-center distance between adjacent micropillars, and D is the micropillar diameter. The micropillar tunnel, which is covered by a sealing block, functions as a check valve for suppressing inverse vapor leakage from the evaporator to the compensation chamber. The microchannel functions as a vapor line, condenser, and liquid line. The latent heat of the generated vapor is released in the microchannel through its condensation.

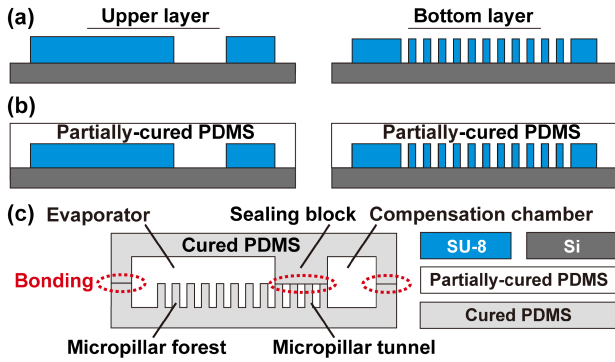


Fig. 2. Fabrication of a micropillar-pumped polymer loop heat pipe using simple, cost-effective soft lithography: (a) preparation of molds, (b) pouring of polydimethylsiloxane (PDMS), and (c) bonding of patterned PDMS films.

TABLE I

PARAMETERS OF THE MICROPILLAR-PUMPED POLYMER LOOP HEAT PIPE

Specifications	Dimensions
Film case	
Length × Width × Thickness	82 mm × 52 mm × 1.8 mm
Weight	7.7 g
Evaporator	
Length × Width × Inner height	12 mm × 20 mm × 0.27 mm
Area of the micropillar forest (Length × Width)	10 mm × 20 mm
Area of the micropillar tunnel (Length × Width)	2 mm × 20 mm
Height and diameter of micropillars	45 μm and 37 μm
Center-to-center distance of micropillars	40 μm
Area of the heater block	10 mm × 20 mm
Compensation chamber	
Length × Width × Inner height	30 mm × 25 mm × 0.27 mm
Microchannel	
Path length × Width × Inner height	213 mm × 3 mm × 0.27 mm

The condensed liquid circulates back to the compensation chamber through the microchannel.

Fig. 2 illustrates the fabrication of the micropillar-pumped polymer LHP. The device is fabricated from polydimethylsiloxane, which is compatible with flexible electronics [13]. The micropillar wick and other components of the polymer LHP are fabricated via soft lithography. First, two molds for the LHP components are prepared using the conventional photolithography process (Fig. 2(a)). One mold holds the patterns of the micropillar wick, compensation chamber, and microchannels. The other mold holds the complementary patterns of the sealing block in the evaporator, compensation chamber, and microchannels. Then, PDMS is poured into both these molds (Fig. 2(b)). After vacuuming the air bubbles from the poured PDMS, the PDMS films are partially cured at 65 °C for 30 minutes and peeled from the molds. The micropillar wick is aligned in the evaporator section with microscale precision. The clearance between the micropillar wick and inner side wall is controlled to prevent vapor leakage. Finally, the upper PDMS film is placed on the surface of the bottom PDMS film and completely cured at 65 °C for 12 hours (Fig. 2(c)). The interface between the top of the micropillars and the sealing block is bonded as PDMS is fully cured. This forms a micropillar tunnel between the evaporator and the compensation chamber, which acts as a check valve as the bonding is sufficiently strong.

III. RESULTS AND DISCUSSION

The proposed design and fabrication approach was demonstrated using a micropillar-pumped polymer LHP. The design parameters of

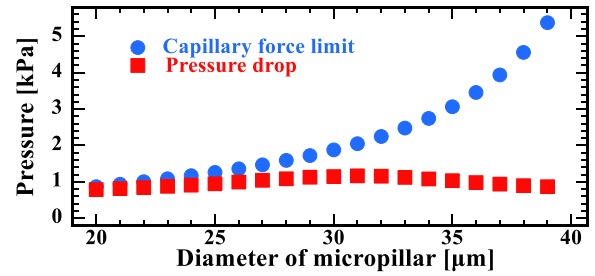


Fig. 3. Calculation result of the pressure drop and the capillary force limit.

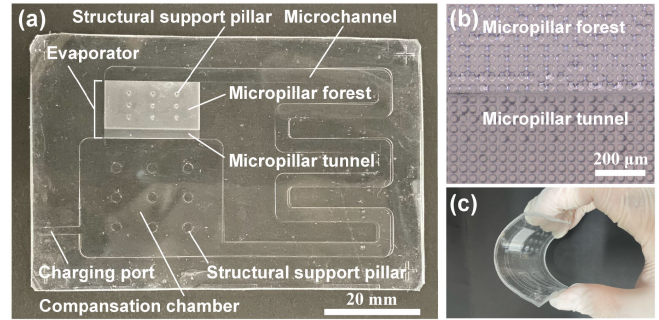


Fig. 4. Fabrication results of the micropillar-pumped polymer loop heat pipe: (a) top view, (b) magnified view of the evaporator, and (c) bending behavior.

the fabricated polymer LHP are given in Table I. The micropillar parameters were determined using (1) to compensate for the pressure drop through the microchannel flow. Fig. 3 shows the calculation result of the pressure drop and the capillary force limit at different diameters when L is 40 μm , and the heat load is 2.0 W. The pressure drop was calculated based on a one-dimensional numerical model which was previously constructed by the authors [9]. In this calculation, the working fluid was ethanol, and the permeability of the micropillar wick was estimated by a numerical model [12]. From Fig. 3, the diameter was chosen to be larger than 35 μm because the capillary force limit was more than three times higher than the pressure drop, considering the safety margin. Fig. 4 presents the fabrication results of the polymer LHP. The evaporator with a micropillar wick, a microchannel, and a compensation chamber were fabricated from PDMS (Fig. 4(a)). The structural support pillars which prevent the fluid flow path to be closed were placed in the evaporator and the compensation chamber. Fig. 4(b) shows a magnified view of the boundary between the micropillar forest and micropillar tunnel. The fabricated device was highly flexible, as illustrated in Fig. 4(c).

To quantify the cooling by latent heat, the operation behavior of the fabricated polymer LHP was compared with that of a non-fluid-charged LHP. Ethanol was selected as the working fluid because of the wettability of PDMS surfaces by ethanol. Ethanol was fully charged into the polymer LHP and then vaporized under heat load to adjust the filling volume. At this time, the charging port remained open. The charging port was then closed using an epoxy resin. Subsequently, the heat load was eliminated. The characteristic of the polymer LHP was evaluated based on its horizontal orientation. A ceramic heater was attached to the bottom side of the evaporator section and the heat load was adjusted within the 0.5–2.5 W range with a step size of 0.25 W. The temperature distribution on the top side of the polymer LHP was captured using a thermography camera (R500EX-pro, Nippon Avionics, Kanagawa, Japan). Ethanol was re-charged at each 0.25 W step owing to the gas permeability of PDMS. An additional coating with a low-permeability material including parylene could be a candidate solution for the long-term operation of the polymer LHP.

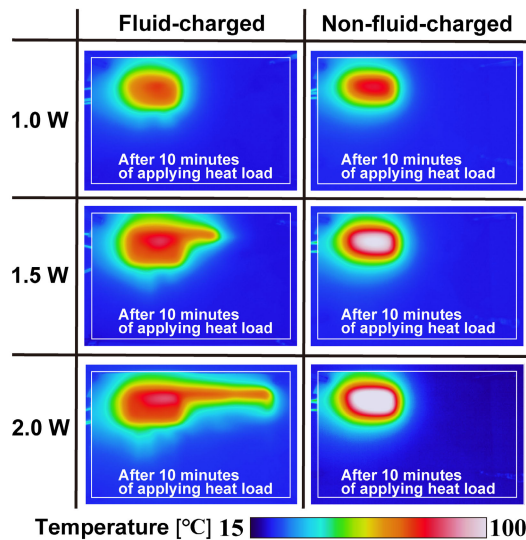


Fig. 5. Thermographic temperature distributions in the fluid-charged and non-fluid-charged loop heat pipes under heat loads of 1.0, 1.5, and 2.0 W.

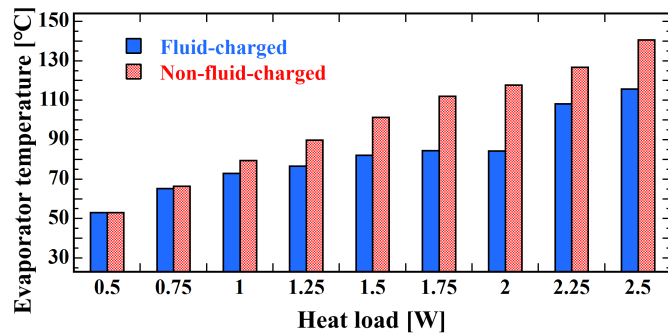


Fig. 6. Evaporator temperatures of the fluid-charged and non-fluid-charged loop heat pipes under different heat loads.

Fig. 5 shows the steady-state temperature distributions in the fluid-charged and non-fluid-charged LHPs under heat loads of 1.0, 1.5, and 2.0 W. Each case was imaged after 10 minutes of applying the heat load. In the non-fluid-charged LHP, heat was transported only via conduction. In the fluid-charged LHP, at 1.5 W heat load, vapor transport began along the vapor line, resulting in a temperature rise along the vapor line. The temperature rise in the evaporator section of the fluid-charged LHP was less than that of the non-fluid-charged LHP. This was because of the latent heat of the liquid which was continuously pumped by the micropillar wick from the compensation chamber to the evaporator. At a 2.0 W heat load, the vapor in the fluid-charged LHP reached the other side of the microchannel, showing that heat was transported over a distance of 38 mm. No clear temperature rise was observed in the compensation chamber, revealing that the micropillar tunnel successfully suppressed inverse vapor leakage.

Fig. 6 shows the maximum temperatures in the evaporator section that were extracted from the thermographic images at 0.5–2.5 W

heat load. The evaporator temperature is defined as the maximum temperature in the evaporator section. At 1.0 W heat load, the temperatures in the fluid-charged and non-fluid-charged LHPs began diverging when vapor began growing in the evaporator section. The temperature difference increased at higher heat loads and reached ~ 34 °C at 2.0 W heat load. The maximum temperature of the fluid-charged LHP abruptly jumped at 2.25 W heat load as the micropillar wick began drying, thus lowering the cooling effect. The fabricated LHP decreased the temperature by up to 34 °C compared to that of the non-fluid-charged LHP and functioned as a passive two-phase heat transfer device. Future works will focus on the additional coating for the long-time stability and the operation test at different bending angles.

REFERENCES

- [1] C. Oshman, Q. Li, L.-A. Liew, R. Yang, V. M. Bright, and Y. C. Lee, "Flat flexible polymer heat pipes," *J. Micromech. Microeng.*, vol. 23, no. 1, Jan. 2013, Art. no. 015001, doi: [10.1088/0960-1317/23/1/015001](https://doi.org/10.1088/0960-1317/23/1/015001).
- [2] Y.-H. Lin, S.-W. Kang, and T.-Y. Wu, "Fabrication of polydimethylsiloxane (PDMS) pulsating heat pipe," *Appl. Thermal Eng.*, vol. 29, nos. 2–3, pp. 573–580, Feb. 2009, doi: [10.1016/j.applthermaleng.2008.03.028](https://doi.org/10.1016/j.applthermaleng.2008.03.028).
- [3] C. Liu, Q. Li, and D. Fan, "Fabrication and performance evaluation of flexible flat heat pipes for the thermal control of deployable structure," *Int. J. Heat Mass Transf.*, vol. 144, Dec. 2019, Art. no. 118661, doi: [10.1016/j.ijheatmasstransfer.2019.118661](https://doi.org/10.1016/j.ijheatmasstransfer.2019.118661).
- [4] J. Lim and S. J. Kim, "Fabrication and experimental evaluation of a polymer-based flexible pulsating heat pipe," *Energy Convers. Manage.*, vol. 156, pp. 358–364, Jan. 2018, doi: [10.1016/j.enconman.2017.11.022](https://doi.org/10.1016/j.enconman.2017.11.022).
- [5] C. Oshman, "The development of polymer-based flat heat pipes," *J. Microelectromech. Syst.*, vol. 20, no. 2, pp. 410–417, Apr. 2011, doi: [10.1109/JMEMS.2011.2107885](https://doi.org/10.1109/JMEMS.2011.2107885).
- [6] C. Oshman et al., "Thermal performance of a flat polymer heat pipe heat spreader under high acceleration," *J. Micromech. Microeng.*, vol. 22, no. 4, Apr. 2012, Art. no. 045018, doi: [10.1088/0960-1317/22/4/045018](https://doi.org/10.1088/0960-1317/22/4/045018).
- [7] P. Szymanski, R. Law, R. McGlen, and D. Reay, "Recent advances in loop heat pipes with flat evaporator," *Entropy*, vol. 23, no. 11, p. 1374, Oct. 2021, doi: [10.3390/e23111374](https://doi.org/10.3390/e23111374).
- [8] P. H. D. Santos, E. Bazzo, S. Becker, R. Kulenovic, and R. Mertz, "Development of LHPs with ceramic wick," *Appl. Thermal Eng.*, vol. 30, no. 13, pp. 1784–1789, Sep. 2010, doi: [10.1016/j.applthermaleng.2010.04.010](https://doi.org/10.1016/j.applthermaleng.2010.04.010).
- [9] N. Watanabe, T. Mizutani, and H. Nagano, "High-performance energy-saving miniature loop heat pipe for cooling compact power semiconductors," *Energy Convers. Manage.*, vol. 236, May 2021, Art. no. 114081, doi: [10.1016/j.enconman.2021.114081](https://doi.org/10.1016/j.enconman.2021.114081).
- [10] K. Nakamura, A. Ueno, and H. Nagano, "Experimental study on long-distance anti-gravity loop heat pipe with submicron-scale porous structure," *Appl. Thermal Eng.*, vol. 214, Sep. 2022, Art. no. 118793, doi: [10.1016/j.applthermaleng.2022.118793](https://doi.org/10.1016/j.applthermaleng.2022.118793).
- [11] A. Ueno, S. Tomita, and H. Nagano, "Experimental investigation on a thin-loop heat pipe with new evaporator structure," *J. Heat Transf.*, vol. 143, no. 6, Jun. 2021, Art. no. 06190, doi: [10.1115/1.4050405](https://doi.org/10.1115/1.4050405).
- [12] S. Adera, D. Antao, R. Raj, and E. N. Wang, "Design of micropillar wicks for thin-film evaporation," *Int. J. Heat Mass Transf.*, vol. 101, pp. 280–294, Oct. 2016, doi: [10.1016/j.ijheatmasstransfer.2016.04.107](https://doi.org/10.1016/j.ijheatmasstransfer.2016.04.107).
- [13] L. Zhang, C. Zhang, Z. Tan, J. Tang, C. Yao, and B. Hao, "Research progress of microtransfer printing technology for flexible electronic integrated manufacturing," *Micromachines*, vol. 12, no. 11, p. 1358, Nov. 2021, doi: [10.3390/mi12111358](https://doi.org/10.3390/mi12111358).